Contrib Mineral Petrol (2007) 153:339–353
DOI 10.1007/s00410-006-0150-z

ORIGINAL PAPER

Magmatic graphite in dolomite carbonatite at Pogranichnoe, North Transbaikalia, Russia

A. G. Doroshkevich · F. Wall · G. S. Ripp

Received: 26 April 2006 / Accepted: 9 October 2006 / Published online: 9 November 2006

Abstract A recently discovered dolomite carbonatite at Pogranichnoe, North Transbaikalia, Russia, dated at 624 ± 3 Ma, contains xenoliths of calcite-bearing dolomite carbonatite with graphite spherulites. Apatite and aegirine are the other rock-forming minerals. Chemically the carbonatites are ferrocarbonatite and ferruginous calciocarbonatite. The graphite forms <1 mm up to 1.5 mm diameter spherulites, with Raman spectra similar to published spectra of microcrystalline, amorphous carbon and disordered graphite, with G and D bands at 1,580–1,600 cm^{-1} and at around 1,350 cm^{-1}. Alteration has formed Fe-bearing calcite to Ca-bearing siderite compositions not previously reported in nature around the graphite along cracks and fractures. Mineral and stable isotope geothermometers and melt inclusion measurements for the carbonatite all give temperatures of 700°–900°. It is concluded that the graphite precipitated from the ferrocarbonatite magma. There are three candidates to control the precipitation of graphite (a) a redox reaction with Fe^{II} in the magma, (b) potential presence of organics in the magma (c) seeding of, or dissolution in, the magma of graphite/diamond from the mantle, and further work is required to identify the most important mechanism(s). Graphite in carbonatite is rare, with no substantial published accounts since the 1960s but graphite at other localities seems also to have precipitated from carbonatite magma. The precipitation of reduced carbon from carbonatite provides further evidence that diamond formation in carbonate melts at high mantle pressures is feasible.

Keywords Dolomite carbonatite · Graphite · Transbaikalia

Communicated by J. Hoefs.

A. G. Doroshkevich · G. S. Ripp
Geological Institute SB RAS, Sakhanovoy st., 6a,
Ulan-Ude, 670047, Russia
e-mail: ripp@gin.bsc.buryatia.ru

G. S. Ripp
e-mail: ripp@gin.bsc.buryatia.ru

F. Wall (✉)
Department of Mineralogy, The Natural History Museum,
Cromwell Road, London, SW7 5BD, UK
e-mail: f.wall@nhm.ac.uk

Introduction

A new area of carbonatites has been discovered recently in North Transbaikalia, Russia (Ripp et al. 2003, 2005). It consists of two carbonatite occurrences called Pogranichnoe and Veseloe in the area of the Uakit and Kelyana river basins and the western border of the Parama depression (Fig. 1). The Transbaikalia carbonatites have some distinct and unusual features such as the absence of comagmatic alkaline silicate rocks, the presence of graphite spherulites (at Pogranichnoe), high Cr-xenoliths (at Veseloe), an order crystallization from dolomite to calcite-rich carbonatite (the classic sequence is calcite carbonatite, through dolomite carbonatite to ankeritic or sideritic carbonatites) and δ^{13} C values higher than many other carbonatites worldwide. They have been proposed as candidates for direct mantle-derived carbonatite magmas (Ripp et al. 2003, 2004, 2006). This paper concentrates on Pogranichnoe in order to report rare graphite-bearing carbonatites.

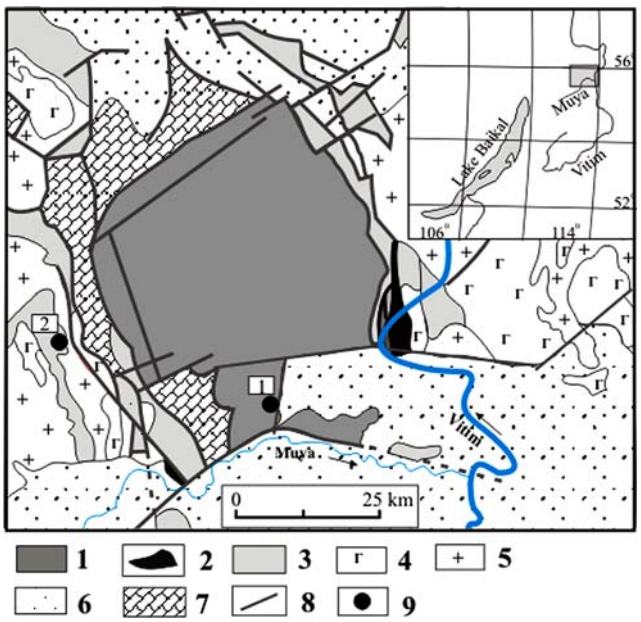

Fig. 1 Schematic geological map of the East Muya area (modified after Dobretsov and Bulgatov 1991). *1* Pre-Cambrian crystalline basement (North-Muya block); *2* ultrabasic rocks; *3* metavolcanic rocks; *4* gabbros; *5* granites; *6* Cambrian sedimentary deposits; *7* Late Riphean limestones; *8* faults; *9* Pogranichnoe (1) and Veseloe (2) carbonatites

Geological description of the Pogranichnoe area

Pogranichnoe is situated in the south of the North-Muya block in Precambrian crystalline basement (Fig. 1; Dobretsov and Bulgatov 1991). Late Riphean gabbros and granites intrude crystalline biotite and amphibole-biotite slates, gneisses, granite-gneisses and marble and all rocks have undergone progressive metamorphism to amphibolite and epidote-amphibolite facies. The carbonatites are situated in a fault zone along the western border of the Parama depression (Fig. 2) along which the basic and sedimentary-metamorphic country rocks are strongly mylonitized and the carbonatites also have intense fissuring.

Carbonatites

The carbonatite outcrop consists of a steeply dipping body elongated East–West, 30–100 m wide and over 450 m long (Fig. 2). A date of 624±3 Ma has been obtained by Ar/Ar dating of arfvedsonite containing 1.7 wt.% K_2O (Ripp et al. 2005).

There are two phases of carbonatite. The main phase carbonatite comprises over 90% of the intrusion and consists of massive medium-grained calcite-bearing dolomite carbonatite. It contains xenoliths of an earlier 'first phase' dolomite carbonatite that is rich in magnetite and contains graphite spherulites. These xenoliths vary from less than a centimetre to a few metres in diameter. The boundaries between the first and main phase carbonatites are difficult to distinguish on fresh surfaces but are clear on weathered surfaces where the first phase carbonatite weathers orange-brown and the main phase carbonatite is a paler grey-brown.

The main phase carbonatite also contains many xenoliths of country rock (slates and gabbros from <1 cm to 1 m diameter), particularly in brecciated areas in the contact zones. The surface of some xenoliths is covered with a thin shell of biotite and they are usually fenitized. There are no xenoliths in the 'first phase' carbonatites.

A few metres of fenitized country rock, containing aegirine, arfvedsonite, albite, biotite and K feldspar with accessory magnetite, titanite and apatite occurs around the carbonatite intrusion.

Analytical methods

Whole rock chemistry was determined by atomic absorption, with trace element determinations by XRF and REE by ICP-AES with preliminary chemical concentration. For REEs certified standard apatite ore

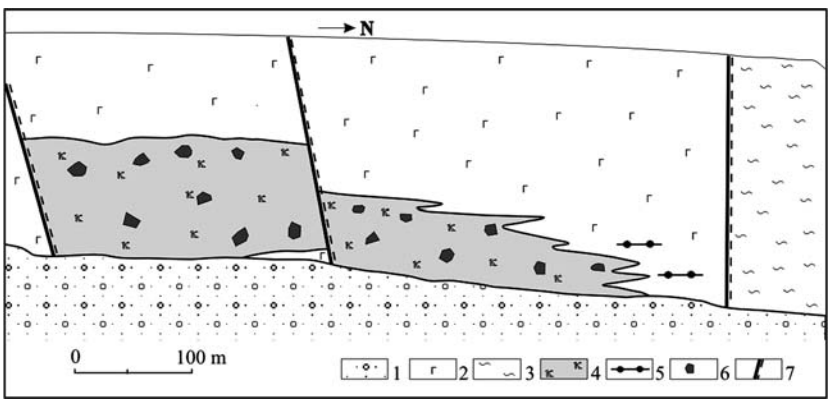

Fig. 2 Schematic geological map of Pogranichnoe. *1* Loose recent deposits; *2* gabbro, gabbro-dolerite; *3* crystalline slate; *4* carbonatite, *5* dykes of alkaline syenite; *6* xenoliths of country rocks; *7* fault

(AR) and apatite (AK) were used as quality control standards.

The minerals were analysed using electron probe micro-analysis (EPMA). Most analyses were carried out at the Geological Institute SB RAS using a MAR-3 WDS microprobe with an accelerating voltage of 20 kV, beam current of 40 nA, beam size of 3–4 μm and a 20 s counting time and a LEO-1430 scanning electron microscope with an IncaEnergy-300 energy-dispersive system (SEM-EDS) operated at 20 kV and 0.5 nA. Additional imaging and analyses were carried out at the Natural History Museum, London using a Jeol 5900 LV SEM equipped with an Oxford INCA EDS system and operated at 15 kV and 1 nA specimen current measured on a Co standard, calibrated with various natural and synthetic materials and using a ZAF matrix correction plus a Cameca SX50 WDS electron microprobe operated at 15 kV and 20 nA (carbonates) and 20 kV and 20 nA (oxides, silicates, phosphates). The beam size was varied from 1 (oxides and small grains) to 20 μm (carbonates) depending on grain size and susceptibility to beam damage. A variety of natural and synthetic materials were used as primary and quality control standards. Matrix correction was by the PAP $\phi\rho z$ method. Cathodoluminescence (CL) was carried out on the JEOL 5900 LV SEM using a Gatan detector for monochromatic imaging.

The $\delta^{13}C$ and $\delta^{18}O$ isotope values were analysed in the isotope laboratory of the Analytical Center FESC RAS (Vladivostok, Russia) using a Finnigan MAT 252 sensitive mass-spectrometer. The analytical errors were not more than ±0.05 for carbonates, ±0.1 for graphite and ±0.5‰ for magnetite.

The Raman spectra of graphite spherulites were studied by Ramanor U1000 microspectrometer at 514.5 μm with an Ar^{+}-laser and using a KBr pellet at UIGGM SD RAS (Novosibirsk). Further microRaman spectra, from core to rims of graphite spherulites with 40 μm steps were obtained at Kingston University by a Renishaw 5400 Series Raman Micro Spectrometer with a CCD detector and 514.5 Ar ion laser. The system was operated in confocal mode with the laser focused through the objective lenses (× 20 and × 40) of an Olympus petrological microscope.

Fluid inclusions were studied in polished plates up to 0.3 mm thick. For thermometric studies of inclusions, we used a chamber with a 'silit' heater equipped with an MBI-6 microscope, a V7-40 milivoltmeter, and Pt/Pt-Rh thermocouple calibrated against the melting points of six chemically pure substances and the homogenization temperature of two fluid inclusions synthesized at specified P and T. The calibration curve deviated from the experimental points by no more than 4°C. The rate of sample heating varied, on average, within 5°C/min. Chemical analysis of solid daughter phases was carried out on an MAR-3 WDS electron microprobe (operated at 20 kV, a beam current of 40 nA, a beam size of 3–4 μm and 20 s counting time) and scanning electron microscopy (LEO-1430) with energy-dispersive spectrometry (IncaEnergy-300) (SEM-EDS) operated at 20 kV and 0.5 nA.

Petrography and mineralogy of carbonatites

First phase graphite-bearing dolomite carbonatite

Ferroan dolomite with 5.4–9.77 wt.% FeO comprises up to 50–70 modal% of this carbonatite, forming 1–3 mm grains, often in intergrowths with magnetite and apatite (Table 1, an. 5–8). Sometimes the dolomite is altered along microcracks, rims and cleavages and contains less SrO and more FeO (Table 1, an. 13–15). Fine dispersions of strontianite occur in these areas suggesting the Sr is liberated from the dolomite but not removed.

Magnetite occurs as octahedral crystals and sometimes idiomorphic grains dispersed within the dolomite aggregate, much of which it predates. Crystals are 3–5 mm diameter and comprise 10–15 modal%. The magnetite contains solid inclusions of dolomite and apatite. Pyrite and hematite replace magnetite along cracks and edges of the grains. The composition is pure Fe_3O_4, in contrast to magnetite in many carbonatites, which contains Ti.

Fluorapatite occurs as relatively uniformly distributed lenticular grains (up to 1.5 mm, 2% to 10 modal%) which have 1.5–4.2 wt.% RE_2O_3, 5.16 wt.% SrO and a trace of SO_3. The REE substitute according to the ''belovite scheme''. Solid inclusions of monazite and strontianite occur along cleavages and on rims and microcracks (Fig. 3d).

Aegirine occurs as small euhedral crystals. It does not contain any inclusions of other minerals and is replaced along cracks and at grain edges by arfvedsonite, biotite and magnetite. The amount of aegirine end member is 80–100%, jadeite end member 3–16% and diopside end member less than 5–7% (Table 2). In contrast to aegirine from fenite, the aegirine from the carbonatite has lower Mg and higher Na (Table 2). Aegirine from fenite has diopside up to 30–35% and jadeite less than 3%.

Primary melt inclusions in aegirine

Aegirine contains single primary melt inclusions (Doroshkevich and Ripp 2004), which have homoge-

Table 1 Chemical composition of calcite and dolomite from Pogranichnoe carbonatites

	Calcite I		Calcite II		Dolomite first phase				Dolomite main phase				Altered dolomite		
	1	2	3	4	5	6	7	8	9	10	11	12	13	14	15
Weight percent oxides															
CaO	49.21	52.56	46.67	44.01	26.92	25.17	27.52	27.00	27.99	28.67	29.16	29.33	27.83	27.62	30.93
MgO	1.15	0.58	1.32	2.05	14.76	14.03	15.05	15.05	13.41	12.89	14.22	14.34	13.62	11.21	9.28
MnO	1.40	1.08	1.13	0.80	2.89	2.25	2.87	2.78	1.96	2.14	1.85	1.83	1.70	2.03	1.80
FeO	2.29	1.56	4.68	8.23	5.90	9.77	6.57	6.95	10.04	11.10	9.03	8.99	10.44	13.46	11.96
SrO	2.64	2.04	1.64	1.37	3.18	3.60	2.91	2.93	1.29	1.17	1.38	1.17	0.82	0.35	0.37
Total	56.69	57.82	55.44	56.46	53.65	54.82	54.90	54.71	54.69	55.97	55.64	55.66	54.41	54.67	54.34
Molar%															
$MgCO_3$	2.40	1.21	2.76	4.28	30.85	29.32	31.45	31.45	28.03	26.94	29.72	29.97	28.47	23.43	19.40
$CaCO_3$	87.59	93.56	83.07	78.34	47.92	44.80	48.95	48.06	49.82	51.03	51.90	52.21	49.54	49.16	55.06
$MnCO_3$	2.27	1.75	1.83	1.30	4.68	3.65	4.65	4.50	3.18	3.47	3.00	2.96	2.75	3.29	2.92
$FeCO_3$	3.69	2.51	7.53	13.25	9.50	15.73	10.58	11.19	16.16	17.87	14.54	14.47	16.81	21.67	19.26
$SrCO_3$	3.75	2.90	2.33	1.95	4.52	5.11	4.13	4.16	1.83	1.66	1.96	1.66	1.16	0.50	0.53
Total	99.70	101.93	97.53	99.11	97.46	98.61	99.76	99.37	99.02	100.97	101.12	101.28	98.73	98.05	97.15

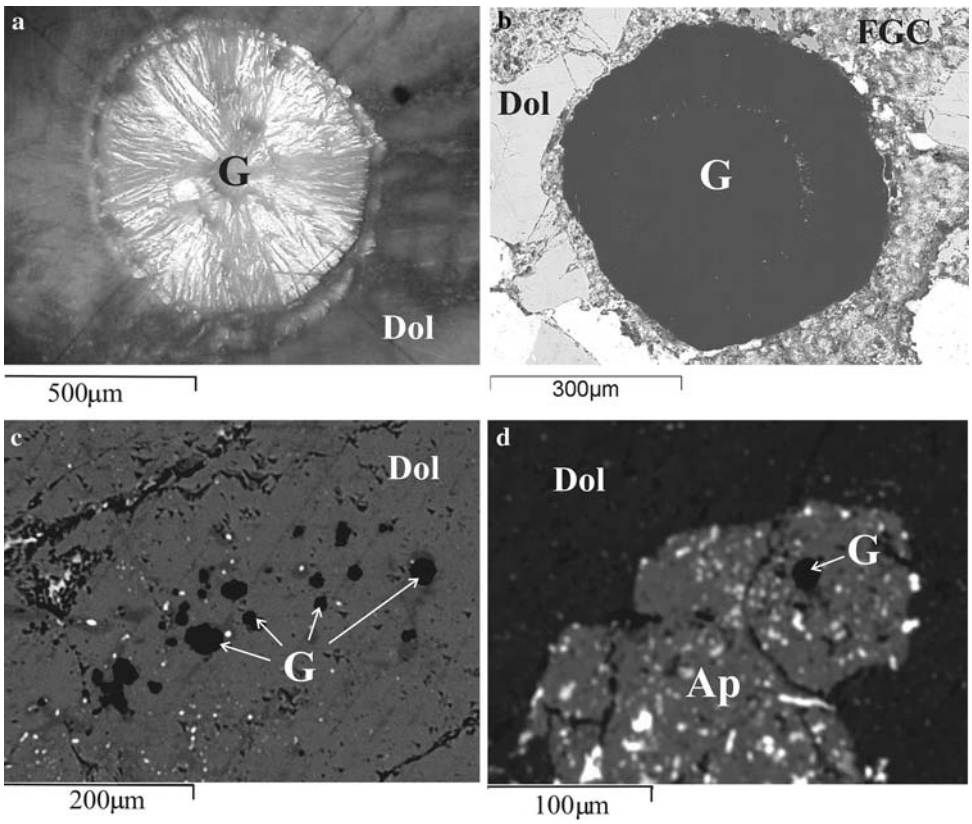

Fig. 3 (**a**) Graphite spherulites with radial structure and ''standing cross'' figure under crossed nicols; (**b**) fine-grained calcite-siderite series carbonates sometimes accompany graphite and fill fracture zones; graphite inclusions in dolomite (**c**) and apatite (**d**). *Dol* dolomite, *FGC* fine-grained carbonate, *G* graphite, *Ap* apatite

nization temperatures above 920°C. At 920°C, the inclusions contained up to 20 vol.% solid but they became opaque at higher temperatures. Among the daughter phases were pyroxene (Cr up to 1 wt.%), K feldspar, dolomite (SrO up to 3 wt.%), carbonates of Ca, Fe, Sr, Ba and REE, and an unidentified phase, consisting of Si, Fe, Na, Ca, K, Ti and Al.

The inclusions were heated up to 1,000°C and then hardened and analysed. The average composition (from 18 analyses) is SiO_2—40.48, Al_2O_3—5.23, FeO—19.62, MgO—2.53, CaO—8.50, Na_2O—4.57, K_2O—0.85, SrO—2.15, P_2O_5—0.66, total—84.61 wt.%, similar to mantle-derived carbonated silicate liquids found in melt inclusions and kimberlitic groundmass (Nielsen et al. 1997; Kamenetsky et al. 2004; Panina 2005) but with higher FeO. This is consistent with the iron-rich composition of the carbonatites. Recalculation of the mineral components produces predominant

Table 2 Chemical composition of pyroxene, amphibole and biotite from Pogranichnoe carbonatite and fenite

	Aegirine								Mg-arfvedsonite						Biotite			
	1	2	3	4	5	6	7	8	9	10	11	12	13	14	15	16	17	18
Weight percent oxides																		
SiO_2	53.04	50.95	52.15	52.83	52.16	52.45	52.49	53.49	51.38	53.07	52.41	52.09	52.46	52.83	54.10	36.04	35.97	40.13
TiO_2	0.17	1.36	0.32	0.37		0.08	0.17	0.14	0.94	0.86	1.19	0.99	0.76	0.54		2.62	3.13	1.04
Al_2O_3	0.67	1.32	2.05	2.28	1.30	2.65	2.81	3.40	2.55	1.89	2.71	2.45	1.80	1.32	1.81	14.31	14.00	11.09
FeO	26.15	24.93	23.97	24.05	29.07	27.43	26.45	25.81	16.18	15.47	17.38	16.62	15.21	22.43	12.45	18.95	18.64	11.78
MnO	0.15	0.21	0.24	0.26		0.07	0.06	0.08	0.38	0.39	0.37	0.31	0.33	0.26	0.18	0.13	0.16	0.07
MgO	2.78	2.79	2.93	2.67	0.40	0.41	0.58	0.56	13.26	14.02	12.39	13.06	13.91	10.82	16.50	12.86	13.10	20.28
CaO	4.77	4.03	5.09	4.74	0.60	0.56	0.96	0.97	2.42	2.18	2.42	2.34	2.52	1.80	2.39			0.04
Na_2O	11.34	12.42	11.47	11.35	13.83	13.58	13.40	13.73	8.25	7.88	7.98	8.42	8.31	8.10	8.01	0.34	0.31	
K_2O								0.03	1.69	1.58	1.61	1.74	1.48	0.95	1.81	9.41	9.56	9.95
F									1.11	1.01	0.95	0.95	1.66	1.59	1.86	1.54	1.33	2.00
Total	99.08	97.99	98.22	98.55	97.36	97.23	97.00	98.19	98.15	98.34	99.40	98.96	98.44	100.62	99.69	96.20	96.20	96.38
–F = O									0.47	0.42	0.40	0.40	0.70	0.67	0.78	0.65	0.56	0.84
Structural formulae based on Si (2). O (6) for aegirine; on O (23). (F+OH)=1 for Mg-arfvedsonite; on O (11). (F + OH) = 2 for biotite																		
Si	2.000	2.000	2.000	2.000	2.000	2.000	2.000	2.000	7.676	7.828	7.724	7.710	7.800	7.876	7.875	2.772	2.759	2.983
Ti	0.005	0.040	0.010	0.010		0.002	0.005	0.004	0.105	0.096	0.132	0.110	0.084	0.060		0.152	0.182	0.058
Al	0.030	0.061	0.093	0.102	0.059	0.119	0.126	0.150	0.450	0.328	0.470	0.427	0.316	0.232	0.310	1.296	1.272	0.972
Fe	0.824	0.818	0.769	0.761	0.932	0.875	0.843	0.807	2.022	1.909	2.141	2.057	1.891	2.797	1.515	1.222	1.209	0.732
Mn	0.005	0.007	0.008	0.009		0.003	0.002	0.003	0.048	0.049	0.046	0.039	0.042	0.033	0.022	0.008	0.011	0.005
Mg	0.156	0.163	0.167	0.151	0.023	0.023	0.033	0.031	2.952	3.083	2.722	2.881	3.084	2.404	3.579	1.475	1.491	2.247
Ca	0.193	0.169	0.209	0.192	0.025	0.022	0.039	0.038	0.387	0.344	0.382	0.371	0.402	0.287	0.372			0.003
Na	0.829	0.945	0.853	0.834	1.028	1.004	0.990	0.995	2.389	2.255	2.281	2.416	2.396	2.340	2.261	0.051	0.047	
K								0.001	0.322	0.297	0.302	0.328	0.280	0.180	0.335	0.928	0.929	0.944
F									0.524	0.469	0.441	0.445	0.781	0.749	0.856	0.376	0.327	0.470
OH									0.476	0.531	0.559	0.555	0.219	0.251	0.144	1.624	1.673	1.530

1–4, 9–12, 16—from fenites. Others from carbonatites. Totals for amphibole and biotite are without H_2O. Detection limits are about 0.05 wt.%

alkaline pyroxene and dolomite. The low analytical total may be related to the presence of carbonate.

Graphite

Graphite forms individual spherulites and sometimes aggregates of 2–4 spherulites and rare platy grains. It is situated between or within grains of dolomite and rarely on the borders of dolomite and magnetite or within magnetite and apatite (Fig. 3c, d). The size of the spherulites varies from <1 mm up to 1.5 mm. The shape of the spherulites is rounded and the surface is knobbly. Sometimes isometric grains show relatively clearly expressed crystallographic octahedral faceting. Under crossed polars most of the spherulite has a radial structure with a ''standing cross'' (Fig. 3a). The cores of some spherulites are granular. Occasionally fine-grained aggregates with varying composition from Fe-bearing calcite to Ca-bearing siderite accompany the graphite and infill fracture zones (Fig. 3b). Parts of the graphite have sharp boundaries with the carbonate matrix but other spherulites have 'friable' borders. The spherulites often contain a concentric zone of carbonate, sometimes with fine plates of hematite. In the outer zones of the spherulites, graphite plates are aligned perpendicular to the surface of the spherulites. Sometimes the spherulite cores contain aggregates of fine-grained Fe-bearing calcite. The δ^{13} C values of the graphite spherulites are discussed below in the isotope geochemistry section.

Raman spectroscopy of the graphite spherulites

The Raman spectra of the Pogranichnoe graphite spherulites are similar to published spectra of microcrystalline, amorphous carbon and disordered graphite, which have G and D bands at 1,580–1,600 cm^{-1} and at around 1,350 cm^{-1} accordingly (Ferrari and Robertson 2001). The first order D and G peaks occur at around 1,360 and 1,582 cm^{-1} and the second order peaks at 2,450, 2,730, 2,944 and 3,252 cm^{-1}. At the edge of the graphite spherulites the 2,450 cm^{-1} peaks are smoothed. In single crystals of Pogranichnoe graphite, the G band occurs at 1,580 cm^{-1}. At Pogranichnoe, there is variation in the intensity of the first and second order G and D bands from the cores to the edges of the

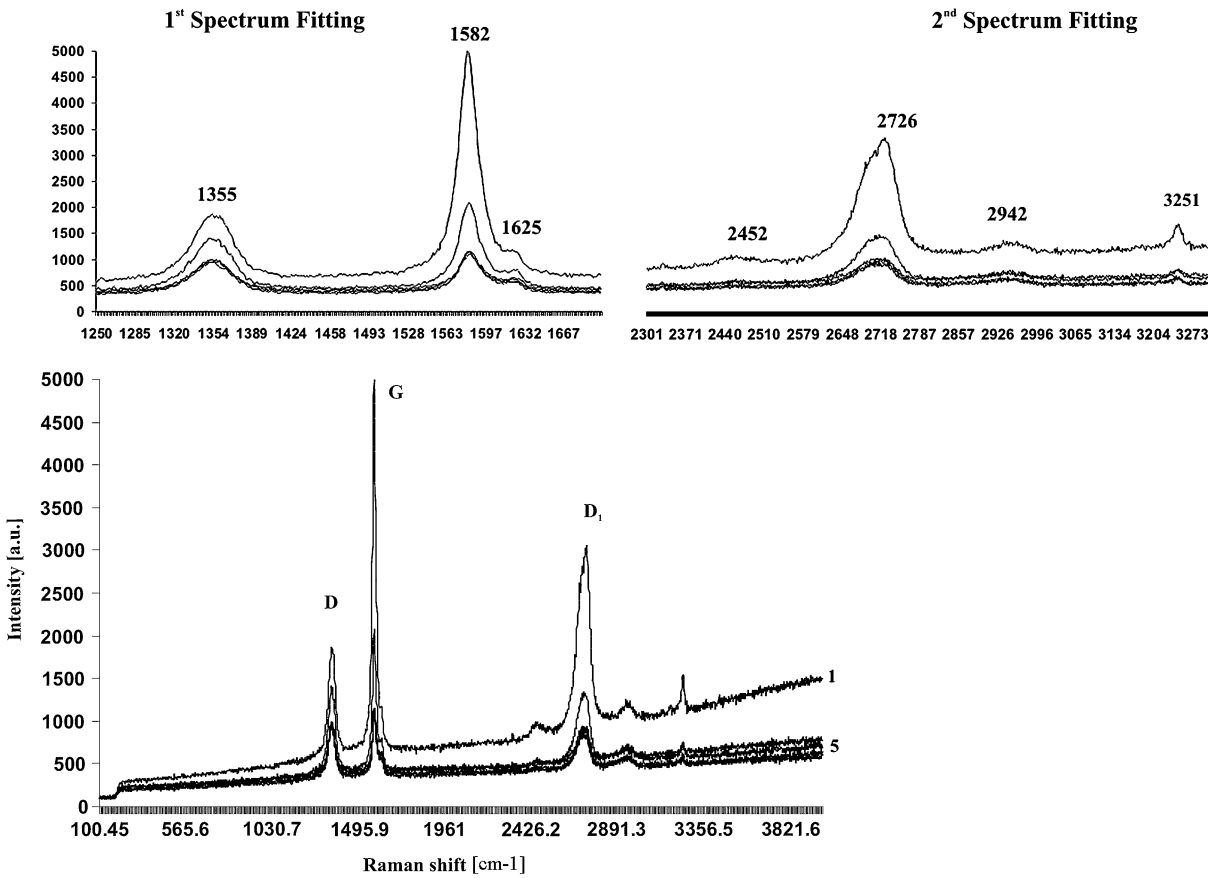

Fig. 4 Raman spectra of graphite spherulites. Representative Raman analyses from core (1) to rim (5) of a spherulite with 40μm steps. *Insets* show regions of the first and second order spectra

spherulites with ratios of 0.35–0.87 (Fig. 4). By comparison with studies of metamorphic graphite this could be interpreted as higher temperature and pressure conditions in the core and lower temperatures and pressures at the rims (Pasteris and Wopenka 1991). The equivalent metamorphic conditions would be garnet zone cores and chlorite zone rims (Wopenka and Pasteris 1993).

Calcite-siderite series carbonates

A distinct set of carbonates fill fracture zones and are associated with graphite (Fig. 3b). They are fine-grained aggregates varying from Fe-bearing calcite to Ca-bearing siderite (Table 3). Such carbonates have not been described previously in nature but have been synthesized at high temperatures (Goldschmidt et al. 1962; Rosenberg 1963). The carbonates also contain high Mg, Mn and Sr and have 7–72% siderite end member, 10–79% calcite end member, 2–16% magnesite end member, up to 13% rhodochrosite end member and up to 5% strontianite end member (Table 3). According to the Goldschmidt diagram (Fig. 5, Goldschmidt et al. 1962) the sub-liquidus temperature of formation of calcite-siderite varies from 400 to 900°C, although the graph does not consider magnesite, rhodochrosite or strontianite end members. It is possible that a primary protomineral dissociated to the fine-grained aggregate. An average overall composition of the mixed carbonate was calculated by multiple SEM/EDS spots. The 'protocarbonate' is CaO—31.85 wt.% FeO—15.3 wt.%, which corresponds to 25% siderite end member (Table 3, analysis 14) and according to the Goldschmidt diagram (Fig. 5, Goldschmidt et al. 1962) corresponds to a sub-solidus temperature of formation of 600°C.

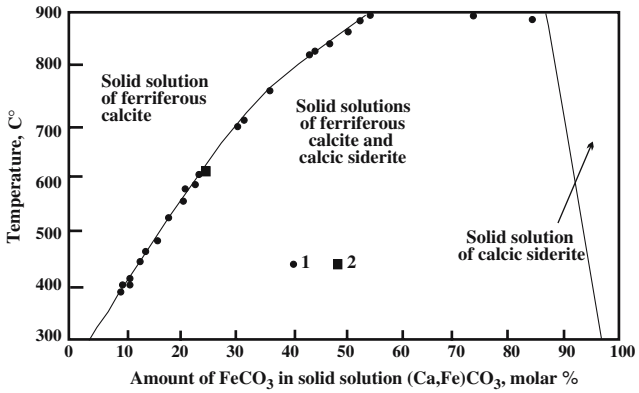

Fig. 5 Sub-solidus temperature of formation the calcite-siderite series carbonates (*1*) and average overall composition of the mixed carbonate (*2*) (calculated by multiple spots on SEM/EDS) plotted on diagram of Goldschmidt et al. (1962)

Dolomite in the contact zone with the fine-grained Fe-bearing calcite has recrystallized producing a dissemination of strontianite, with a resulting decrease in the Sr content of the dolomite from 3–4 down to 0.5 wt.% SrO (see Table 1, an. 13–15). This dolomite alteration and the location of the calcite-siderite carbonates along fracture zones lead to the conclusion that this carbonate is an alteration product. The association with graphite and rarity of the Ca-siderite composition mean that the presence of graphite was probably crucial in producing a reducing environment that enabled these carbonates to form.

Accessory minerals

Pyrochlore, thorite, columbite, monazite-(Ce) and zircon are accessory minerals in both the first and main carbonatites. Monazite-(Ce) occurs as fine dissemina-

Table 3 Composition of calcite-siderite series carbonates from the association with graphite in Pogranichnoe carbonatites

	1	2	3	4	5	6	7	8	9	10	11	12	13	14
Weight percent oxides														
MgO	2.06	1.64	7.73	3.21	1.26	0.98	0.63	0.79	1.81	1.89	3.54	5.54	6.83	5.41
CaO	6.13	43.44	33.38	11.63	28.43	8.25	40.66	44.33	31.49	19.59	18.51	27.47	36.61	31.85
MnO	1.06				2.00	0.98	0.91	1.07	1.23	2.20	2.66	3.22	1.32	3.82
FeO	51.97	8.11	4.81	45.25	25.19	15.08	10.41	6.25	32.31	34.48	33.46	23.21	12.98	15.29
SrO		3.25			2.02	3.10	2.87	3.56	2.02	1.92	1.08		0.45	0.91
Total	61.22	56.44	55.56	60.09	58.87	58.39	55.48	56.02	59.86	60.08	59.25	59.44	58.19	57.28
Molar%														
$MgCO_3$	4.31	3.43	16.16	6.71	2.63	2.05	1.32	1.65	3.26	3.95	7.40	11.24	13.86	11.31
$CaCO_3$	10.91	77.32	59.42	20.70	50.55	68.09	72.37	78.91	48.32	34.87	32.95	47.47	63.27	56.69
$MnCO_3$	1.72				3.24	1.59	1.47	1.73	1.72	3.56	4.31	5.06	2.08	6.19
$FeCO_3S$	83.67	13.04	23.84	72.85	40.56	24.28	16.76	10.06	44.84	55.51	53.87	36.28	20.29	24.62
$SrCO_3$		4.62			2.87	4.40	4.08	5.06	2.47	2.73	1.53		0.62	1.29
Total	100.61	98.41	99.42	100.26	99.85	100.40	96.00	97.41	100.62	100.62	100.06	100.06	100.11	100.10

Analysis 14—average composition of the mixed carbonate (calculated by multiple spots on SEM/EDS). Detection limits are about 0.05 wt.%

tions and solid inclusions in apatite; occasionally also outside magnetite, graphite and apatite. The monazite-(Ce) is strongly light REE-enriched (Ce/La, Ce/Nd and La/Nd average ratios 1.9, 3.3 and 1.9, respectively) with 0.11–0.73 wt.% ThO_2. Small amounts of Ca, Si, Sr, U and Pb are also present.

Main phase dolomite carbonatites

The main phase dolomite comprises the majority of the occurrence. The major differences from the first phase carbonatite are the lack of graphite, finer grained nature of the dolomite, lower amount of magnetite and presence of calcite. The dolomite is again ferroan dolomite but with higher Fe (up to ankerite) and lower Sr (Table 1, an. 9–12). Magnetite single idiomorphic grains, comprise up to 3 modal% and have the same composition as in the first stage carbonatite. Fluorapatite also has the same composition as in the first phase carbonatite but fewer inclusions of monazite. There are two types of calcite, one idiomorphic and associated with dolomite and another in interstices between dolomite (Table 1). Orthoclase phenocrysts contain 5% shoe-string albite perthite. Aegirine has the same composition as the aegirine in the first phase carbonatite (Table 2). Magnesioarfvedsonite is distinct in composition from fenite amphibole (Table 2).

Chemical composition of the carbonatites

The Pogranichnoe carbonatites are chemically ferrocarbonatites and ferruginous calciocarbonatites (Table 4, Fig. 6). They plot in the Fe-rich portion of Fig. 6 because of their high magnetite contents rather than because they contain Fe-rich carbonate. From the earliest to the latest phase the amount of Fe decreases and Ca increases (Fig. 6) as the magnetite content decreases and calcite increases; the amounts of Sr, REE, Nb, Mg and P decrease but HREE and Y do not vary. Silica is usually 1–3 wt.% although the carbonatites are sometimes enriched in Si as a result of the presence of orthoclase, aegirine and secondary quartz.

A comparison with average ferrocarbonatite calculated by Woolley and Kempe (1989) (Fig. 7) emphasizes the high level of Sr (average 2.3 wt.% SrO, maximum 4.2 wt.%), which is 3–4 times higher in Pogranichnoe carbonatites than in average ferrocarbonatite. The Fe, P and Mg contents are also higher than average, and Ti, Zr and S are all lower. The REE content is similar to average ferrocarbonatite and varies from 0.35 to 1.55 wt.% RE_2O_3, with monazite-(Ce) and apatite as the main mineral hosts. LREE are more highly concentrated than HREE three orders of magnitude variation in La/Yb chondrite normalized ratios. Niobium contents are low (from 4 to 35 ppm), three times less than in average ferrocarbonatite.

Comparison with other dolomite carbonatites

Six other dolomite carbonatites are plotted on Fig. 7 for comparison with Pogranichnoe, including the Veseloe dolomite carbonatite from nearby in Transbaikalia that has also been proposed as a direct mantle melt but does not contain graphite (Ripp et al. 2004, 2006); Swartbooisdrif, Namibia (Thompson et al. 2002), which is similar in that it is both magmatic and ferrocarbonatite but proposed to form by immiscibility; Tamazert, Morocco, a carbonatite that carries mantle debris (Mourtada et al. 1997); Shawa and Dorowa dolomite carbonatites where isotopic evidence suggests no direct link between the dolomite carbonatite and associated silicate rocks and direct mantle melts have been proposed (Harmer et al. 1998); and late-stage ancylite-bearing (REE-rich) carbonatites at Sokli, Finland (Lee et al. 2004). Pogranichnoe is not obviously mineralogically or geochemically aligned with any one variety of dolomite carbonatite; it has notably high REE but the REE-rich carbonatites usually form in the final stages of emplacement of a carbonatite complex in a pegmatitic or subsolidus phase (Wall et al. 2001) and this activity is not seen at Pogranichnoe. There are no clear patterns within the dolomite carbonatites and the trace element geochemistry of the dolomite carbonatite does not lead us towards the fundamental reason for the presence of graphite at Pogranichnoe.

Carbon, oxygen and strontium isotope compositions

Initial $^{87}Sr/^{86}Sr$ ratios were determined in a few apatite and dolomite separates and are consistent with a mantle source (Bell and Blenkinsop 1989; Table 5). The isotope compositions of C and O were analysed in mineral separates of dolomite, calcite, apatite, magnetite, graphite and arfvedsonite (Table 5).

The $\delta^{13}C$ values in dolomite and calcite vary from –0.2 to 0.4‰. Average $\delta^{18}O_{VSMOW}$ values for dolomite are 9.12‰ with variations from 8.4 up to 10.18‰. $\delta^{18}O$ values in calcite from dolomite-calcite rocks (latest phase) are higher ($\delta^{18}O$ 11.08‰). The $\delta^{18}O$ value in aegirine (5.3‰$_{VSMOW}$) is similar to mantle-derived silicate minerals, but the value for arfvedsonite (6.3‰$_{VSMOW}$) is higher, which is consistent with arfvedsonite being an alteration product of aegirine during

Table 4 Chemical composition of Pogranichnoe carbonatites

	1	2	3	4	5	6	7	8	9	10	11	12	13	14	15	16	17
Weight percent																	
SiO_2	5.20	2.90	2.38	2.32	1.54	1.90	5.70	1.20	9.60	1.14	5.20	1.40	5.80	1.50	1.14	1.00	1.68
TiO_2	0.09	0.05		0.06		0.05	0.10	0.06	0.12	0.03	0.06	0.05	0.22	0.04		0.04	0.08
Al_2O_3	1.10	0.35	0.21	0.42	0.15	0.40	0.88		3.05	0.14	1.15	0.31	1.35	0.14		0.17	0.40
Fe_2O_3	11.39	10.51															
FeO	9.54	8.86															
FeO total			22.80	18.14	16.98	16.98	20.24	20.89	14.78	18.97	16.85	18.81	18.14	17.64	21.33	16.98	21.33
MnO	1.88	1.77	1.94	1.29	1.59	1.66	1.52	1.55	1.14	1.46	1.71	1.63	1.70	1.75	1.52	1.81	1.53
MgO	7.28	7.33	8.24	7.59	8.00	7.84	7.00	7.89	7.52	8.00	6.16	8.00	6.94	7.47	7.84	7.82	7.21
CaO	28.11	27.31	26.24	28.92	28.92	29.59	27.71	29.30	27.98	29.59	28.65	28.92	27.22	28.92	27.58	28.92	26.10
Na_2O	0.33	0.38	0.05	0.20	0.05	0.11	0.08	0.08	0.11	0.08	0.08	0.14	0.16	0.23	0.27	0.14	0.14
K_2O	0.54	0.07	0.17	0.23	0.08	0.31	0.37	0.03	0.98	0.04	0.87	0.16	0.94	0.09	0.07	0.13	0.20
P_2O_5	3.06	3.46	2.35	3.50	2.87	3.57	3.05	3.98	3.66	3.33	2.34	3.50	2.68	3.06	2.48	4.04	3.44
Ba	0.16	0.56	0.07	0.09	0.08	0.14	0.10	0.10	0.11	0.09	0.09	0.14	0.09	0.17	0.15	0.24	0.55
Sr	1.50	4.30	1.19	1.88	1.94	2.36	1.58	1.64	0.92	1.79	1.29	1.89	2.15	3.53	3.12	4.07	4.50
Σ REE	0.84	1.30	0.41	0.57	0.58	0.47	1.11	0.95	0.42	0.82	0.34	0.32	0.24	0.81	0.40	1.25	1.45
CO_2	24.12	24.65	32.76	32.32	34.08	34.52	29.35	31.66	28.80	32.76	32.21	32.76	30.56	32.54	32.32	31.99	29.46
F	0.23	0.24	0.15	0.27	0.22	0.28	0.24	0.33	0.28	0.29	0.22	0.27	0.33	0.25	0.17	0.29	0.25
S	0.18	0.74	0.14	0.19	0.35	0.32	0.42	0.48	0.30		0.25	0.20	0.17	0.20	0.17	0.64	0.52
Total	95.56	94.78	99.10	97.99	97.43	100.51	99.45	100.13	99.76	98.53	97.47	98.51	98.68	98.34	98.55	99.53	98.84
LOI	30.93	30.04	32.76	32.32	34.08	34.52	29.35	31.66	29.80	33.04	32.21	32.76	30.56	32.54	32.32	31.99	29.46
ppm																	
Y	90	110	85	95	92	110	110	100	90	90	90	77	43	130	120	150	120
Nb	15	16	8	6	6	14	25	14	6	5	7	23	26	24	13	32	28
Rb	15	27	9	6			10			7	8	14	4	6	9		
As				6	14	8	13	20		10	12	11	10	28	15	30	42
Bi			24	27	27	50		22	23	22	50			56	37	23	70
Th			10	10	64		120	130	10	36			13	48	45	210	240
Pb	71	240							12	12		10				80	50
La	2,300	3,700	960	1,200	1,400	1,100	3,000	2,600	1,300	2,200	700	670	520	1,900	870	3,600	4,400
Ce	4,400	6,600	2,100	3,000	3,000	2,600	5,700	4,900	3,000	4,500	1,700	1,600	1,200	4,300	2,000	6,200	7,300
Pr	400	480			240		350	360						400		500	480
Nd	1,400	1,900	850	1,100	990	860	1,800	1,400	1,200	1,300	820	800	480	1,300	700	1,900	2,000
Sm	76	140	110	72	77	91	150	140	110	130	66	84	43	120	77	200	200
Eu	29	30															
Gd	105	100	49	85	66	53	110	64	62	76	52	42	28	84	30	85	86
Er	29	30	14	17	14	13	25	19	16	18	19	15	94	24	13	22	24
Yb	3	4	4		3	4	4	6	5	4	6	4		6	4	7	6

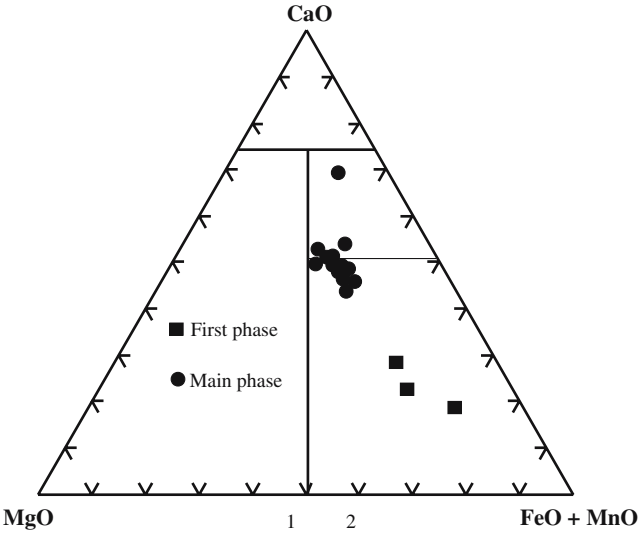

Fig. 6 Pogranichnoe carbonatite whole rock analyses plotted using molar proportions (after Gittins and Harmer 1997). The main phase carbonatites plot in ferruginous calciocarbonatite field owing to the presence of calcite. The first phase does not contain calcite

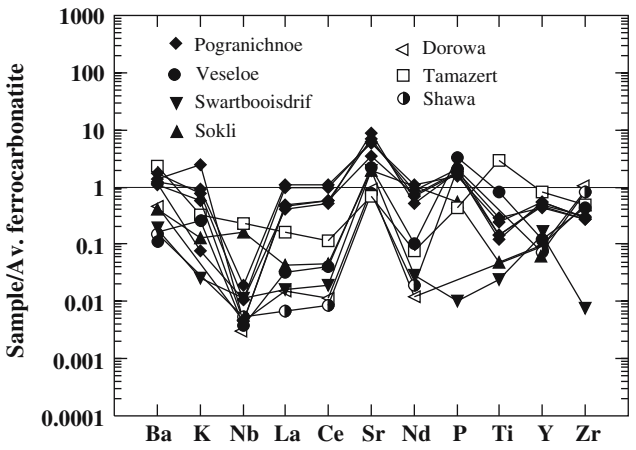

Fig. 7 Comparison of the distribution of selected trace elements in Pogranichoe and other ferroan dolomite and dolomite carbonatites normalized to average ferrocarbonatite (Woolley and Kempe 1989). Data sources are: Veseloe (Doroshkevich et al. 2006), Swartbooisdrif (Thompson et al. 2002), Sokli (Lee 2004), Dorowa (Harmer et al. 1998), Tamazert (Mourtada et al. 1997), Shawa (Harmer et al. 1998)

a late stage process that involved some isotopic exchange (Taylor et al. 1967; Deines 1989; Faure 1986). On Fig. 8, the Pogranichnoe carbonatites show $\delta^{13}C$ values significantly higher than those believed to be representative of mantle-related primary carbonatites (after Taylor et al. 1967; Deines 1989). There is petrographic evidence of minor alteration of dolomite and calcite and associated formation of strontianite, which may account for some of the variation from the 'mantle box'. However, this is minor, and late-stage processes (including Rayleigh fractionation) that affect C also usually affect O in the same way and so it is difficult to explain the Pogranichnoe values that have significantly heavier C but similar O to the currently accepted mantle values.

Table 5 Isotopic composition of O, C and Sr in minerals from Pogranichnoe carbonatites

Carbonatite stage	Analysed material	$\delta^{13}C$‰ VPDB	$\delta^{18}O$‰ VSMOW	$^{87}Sr/^{86}Sr$
First	Dolomite	0.3	10.18	
	Dolomite	0.1	9.4	
	Magnetite		1.04 ± 02	
	Graphite	–6.1± 01		
Main	Dolomite	–0.187	8.41	
	Dolomite	–0.2	9.0	
	Dolomite	0.096	8.6	
	Dolomite			0.70379 ± 1
	Dolomite			0.703817 ± 16
	Apatite			0.70373 ± 1
	Apatite		5.1	
	Magnetite		1.9 ± 0.5	
	Arfvedsonite		6.3	
	Calcite	0.4	11.08	

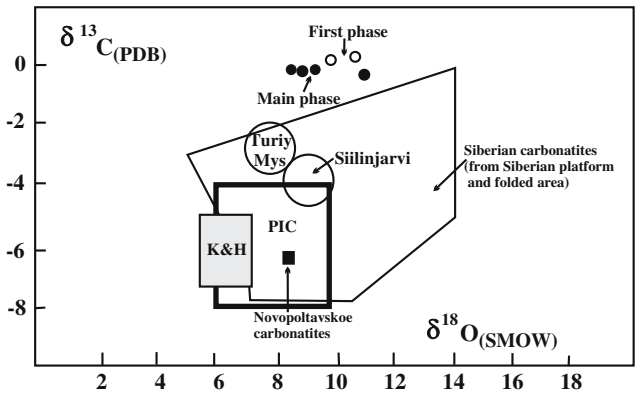

Fig. 8 Stable carbon and oxygen isotope compositions (in ‰ relative to VPDB and VSMOW, respectively) in Pogranichnoe carbonatites. Primary unaltered carbonatites (*PIC*) proposed by Demény et al. (1998) based on Taylor et al. (1967) and Keller and Hoefs (1995) (K&H). Turiy Mys and Siilinjärvi compositions are from Demény et al. (2004), Novopoltavskoe composition is from Lugovaya et al (1980), Siberian carbonatites (Siberian platform and folded area) are from Vladykin et al. (2004)

As distinct from carbonate minerals, the $\delta^{13}C$ values in graphite spherulites (–6.1‰ $\delta^{13}C_{VPDB}$) are compatible with a mantle source; Deines (2002) states that carbon with $\delta^{13}C$ of about –5‰ has been identified as a major isotopic composition signature for the mantle, including carbonatite and kimberlite carbonates, diamonds and volcanic CO_2. The graphite spherulites are also consistent with graphite from carbonatite at

Novopoltavskoe (Ukraine), which has $\delta^{13}C$ values of –6 ± 1.2‰ and was concluded, from the carbon isotope distribution in carbonate and graphite to have formed from a mantle source (Zagnitko et al. 1980). The Novopoltavskoe carbonatites have $\delta^{18}O$ and $\delta^{13}C$ values of 8.2 and –6.1‰ (Fig. 8, Lugovaya et al. 1980). Separated calcite from Novopoltavskoe carbonatites has $\delta^{18}O$ values of 5–13‰ and $\delta^{13}C$ values of –3 to –9‰ (Krivdik 2001).

It is possible to make an estimation of crystallization temperature based on the difference in $\delta^{18}O$ between magnetite (Table 5) and co-existing dolomite (using the calcite-magnetite formula of Chiba et al. 1989). The differences (7.1–6.5‰) correspond to temperatures from 700 to 750°C [determination of the exact temperature value is not possible because the analytical error in $\delta^{18}O$ values in magnetite was high (±0.5‰)]. This seems reasonable and suggests no large disturbance in the O values of the carbonate. A dolomite-graphite thermometer (Wada and Suzuki 1983) corresponds to temperatures from 680 to 700°C.

$\delta^{18}O_{VSMOW}$ for apatite is 5.1‰ and similar to values reported for apatite from carbonatites at Jacupiranga (Santos and Clayton 1995), Angola (Alberti et al. 1999), Penchenga (Vrublevskii et al. 2003) and from the West Transbaikalia carbonatites and apatite-bearing basic rocks (G.S. Ripp, unpublished data).

At about 700°C, the fractionation between graphite and dolomite is 6‰ (Wada and Suzuki 1983). This explains well the variation in the Pogranichnoe carbonatites, and potentially why the carbonate is outside of the accepted mantle PIC box. However, starting with a mantle composition, with graphite at –6‰, the carbonate would have a $\delta^{13}C$ value around 0‰ only if the system was graphite-dominated. The xenoliths contain graphite that seems to be in carbon isotope equilibrium with carbonate but it is not dominant; modal percents of 70% for dolomite and 0.5% for graphite equate to a molar ratio of 10:1 dolomite: graphite. Starting from normal mantle composition, in a carbonate-dominated system, the carbonate would have a $\delta^{13}C$ value of ~–6‰, and the graphite composition would be 6‰ lower. The present data are in agreement with small amount of graphite crystallizing from carbonate melt whose $\delta^{13}C$ value is around 0‰.

Another possible fractionation effect that could cause large changes in C but minor or no movement in O is fractionation in the C–CO–CH (methane and other hydrocarbon)–CO_3 system. C in graphite and methane has lighter values compared to C in carbonate. For example, the isotopic composition of methane from fluid inclusions in kimberlite garnet and olivine (Siberian platform) is –13.2 to –19.3‰ (Kravtsov et al. 1981). The presence of graphite in the first phase carbonatite is evidence of a reducing environment that could have facilitated this effect. The main stage carbonate values are similar, just slightly lighter in C. However, in order to make this change from the 'Primary Igneous Carbonatite' field, *all* of the Pogranichnoe carbonatites would have to have undergone similar fractionation with reduced C species, even though only the first phase carbonatite contains evidence of their presence in the form of graphite. Further work on fluid inclusions is required to investigate this hypothesis.

Other carbonatites that do not contain graphite also have carbonates that plot above the accepted 'PIC' box; for example, $\delta^{13}C$ and $\delta^{18}O$ values in the nearby Veseloe dolomite carbonatites (Doroshkevich et al. 2006), Turiy Mys calcite carbonatites and phoscorites, Russia and Siilinjärvi calcite carbonatite, Finland (Demény et al. 2004). The field for Siberian Platform carbonatites (Fig. 8, Vladykin et al. 2004) also has some similar values. The heavier C values for Turiy Mys carbonatites were described by Dunworth and Bell (2001) and suggested as resulting from isotope exchange with Devonian seawater, or mantle processes (oxidation of diamond by carbonate crystallization) or owing to a specific carbon isotope signature in the mantle. The high $\delta^{13}C$ for Turiy Mys and Siilinjärvi carbonatites were attributed to a decreased amount of CO_2–H_2O fluid associated with the carbonatite magma (Demény et al. 2004). The ^{13}C-enrichment in several early-phase Kola carbonatites was explained by Demény et al. (2004) with mantle metasomatism by slab-derived CO_2, or fractionation by formation and separation of a ^{12}C-enriched phase in the mantle.

Formation of graphite spherulites

Three possible processes of graphite formation are considered here

- graphite picked up from country rocks
- breakdown of Fe carbonate
- precipitation from carbonatite magma

The first case, that the graphite is picked up from country rocks, can be quickly excluded because the country rocks (gabbros and slates) do not contain graphite and the δ^{13} C isotopic composition is not consistent with the organic carbon of sedimentary rocks but is similar to mantle carbon. In addition, graphite only occurs in the smaller volume, first stage carbonatite, whereas country rock xenoliths occur in the surrounding main stage carbonatite.

The formation of graphite as a result of the thermal disproportionation of Fe-carbonate to magnetite with accompanying reduction of the carbonate ion has been investigated by French and Rosenberg (1965) and Weidner and Tuttle (1965). Siderite breaks down and graphite is precipitated from a gas phase.

$$6FeCO_3 \rightleftharpoons 2Fe_32O_4 + CO_2 + C \quad (1)$$

An example was described recently by Zuilen et al. (2003) in metacarbonate rocks from the Isua Supracrustal Belt, West Greenland. A similar scenario for carbonatites was described as long ago as Gellantly (1966) for graphite beads in carbonatites of the Darkainle nepheline syenite complex, Somalia, which are smaller (0.1 mm) but similar in habit to the Pogranichnoe graphite. It is possible that the same mechanism has operated at Pogranichnoe but this scenario does not fit with the petrographic evidence. The magnetite is earlier than dolomite and graphite. There is evidence of a carbonate–graphite reaction along fissures and around some graphite spherules as described above, but this seems to go the other way—the Fe-Ca carbonates have formed by reduction of fluids by the graphite rather than formation of graphite by dissociation of siderite. When we review the detail of the petrography described by Gellantly (1966), we find that the Darkainle carbonatites did not contain a sideritic carbonate but a ferroan dolomite or ankerite that has recrystallized to form dolomite plus limonitic oxides. This kind of change is now known to be very common—ubiquitous in fact—in Fe-bearing dolomitic carbonates, and responsible for their brown colouration (e.g. Wall 2000). Graphite is not usually a by-product of this reaction. Moreover, Gellantly (1966) concludes that owing to the bead-like habit of the graphite and its formation in this habit in experiments, 'the graphite developed while the rock was at least partially molten'. This leads us on to the next option for graphite formation.

This third possibility is that the graphite has precipitated from the carbonatite magma. This hypothesis is consistent with the petrographic evidence of graphite spherulites occurring between dolomite and apatite crystals and as inclusions in dolomite and apatite. The homogenization temperatures of melt inclusions support a high temperature for the carbonatite formation, and the graphite precipitation. This is our favoured hypothesis for Pogranichnoe, and is consistent with the formation proposed for graphite in calcite and dolomite carbonatite at Novopoltavskoe, Ukraine (Zagnitko 1980), and with our slightly revised interpretation of the dolomite carbonatites at Darkainle, Somalia. Other examples of graphite in carbonatite are rare. A brief account of graphite in monazite and magnetite-bearing dolomite carbonatite at Eureka, Namibia was given by Verwoerd (1967) and Worley et al. (1995) and Worley and Cooper (1995) describe graphite in calcite carbonatite of the Dismal nepheline syenite complex, Antarctica. They found graphite in apparent equilibrium with calcite and graphite concentrated at the margin with country rock marble. Isotopic fractionation via the equilibrium $C + O_2 = CO_2$ resulted in enrichment of the ^{13}C isotope in calcite from the nepheline syenite.

The reason for graphite precipitation from the carbonatite magma still requires further testing. In the case of the Dismal nepheline syenite carbonatite, reaction with country rocks seems important. However, there is no obvious wall rock reaction cited in any of the other carbonatite examples. The presence of large amounts of Fe^{II} in the magma is unlikely alone to be the key because then graphite would be expected to occur in phoscorites and associated magnetite-rich carbonatites, such as the Kola Peninsula occurrences (e.g. Krasnova et al. 2004; Lee et al. 2004; Karchevsky et al. 2004) but no graphite has been recorded thus far. Another possibility is the control of the presence of reduced carbon species such as methane, which is more difficult to establish and requires further study of fluid inclusions, but would also account for the carbon isotope signature at Pogranichnoe, as described above.

Evidence from studies of diamond genesis

A link between carbonatitic graphite and diamond is provided by the graphite associated with diamond in calcite silicocarbonatite dykes at Chagatai, Uzbekistan (Djuraev and Divaev 1999). There is also experimental evidence to support graphite precipitation from carbonatite magma in the form of experiments aimed principally at diamond synthesis. Experimental investigations using a multicomponent carbonate-carbon system (Litvin 1998; Litvin et al. 1999; Litvin and Zharikov 2000) and Chagatai carbonatite (Bobrov et al. 2004) have demonstrated spontaneous nucleation and growth of diamond crystals in the diamond PT stability field. Spheroidal graphite crystals were formed by spontaneous nucleation (at conditions when diamond is the thermodynamically stable carbon phase) in one such set of experiments with carbonate-carbon multicomponent melts (Spivak and Litvin 2004).

Several authors have suggested that natural diamonds may form from the carbon of carbonate minerals (Cartigny et al. 2001; Luth 1993; Schrauder and Navon 1994). The synthesis of diamond as a result of

reactions between carbonates and silicates has also been accomplished experimentally (Pal'yanov et al. 2002) and crystallization of metastable graphite under the PT-conditions for diamond stability has been observed for a number of non-metallic systems, such as fluid-containing carbonates and C–O–H fluids (Akaishi et al. 2000; Pal'yanov et al. 1999). These experiments support the hypothesis that the Pogranichnoe graphite precipitated from carbonatite melt and that the occurrence of magmatic graphite in carbonatites provides a natural example of precipitation of reduced carbon from carbonate magmas, lending further circumstantial support to the precipitation of diamonds from carbonate melts at high pressure and temperature in the mantle.

The experiments that produce diamond and graphite from carbonate-bearing magma start doped with diamond. It is possible to envisage some carbonatites originating from, or travelling through, a graphite or diamond-bearing mantle—such as seen in the rocks of Beni Bousera (Pearson et al. 1989)—dissolving excess carbon and then precipitating it rapidly later after travelling to the crust. If the carbonatite is generated in a graphite-rich layer, the system would be graphite-dominated and the carbonate melt would have a ~6‰ higher $\delta^{13}C$ value, equivalent to the values observed for Pogranichnoe. For example CO_2–H_2O metasomatism may cause carbonatite melt generation through low-degree partial melting and thus LREE and Sr enrichment.

Conclusions

1. Graphite spherulites precipitated from ferroan dolomite carbonatite magma at Pogranichnoe at temperatures of at least 700–900°C.
2. Alteration of the carbonate along fractures and in contact with graphite produced siderite-calcite series carbonates previously unreported in nature.
3. Mineral and isotope geothermometers and melt inclusion data from the Pogranichnoe carbonatites confirm the 700–900°C high temperature of rock formation. However, the geochemistry of the carbonatite is not distinct from other dolomite carbonatites.
4. We have identified three candidates for the control on precipitation of graphite (a) a redox reaction with Fe^{II} in the magma, (b) potential presence of organics in the magma (c) seeding of, or dissolution in, the magma of graphite/diamond from a mantle region rich in reduced carbon. More work is required on this and other graphite-bearing carbonatites in order to identify the most important mechanism(s). The presence of graphite itself does not necessarily require direct or rapid mantle derivation, although mechanism (c) would be much more likely with rapid rise from the mantle.
5. Graphite carbonatites have received little recent attention but are potentially useful indicators of conditions in carbonate magmas and potential analogues for diamond precipitation from carbonate melts in the mantle.

Acknowledgments We are grateful to Tony Wighton, John Spratt, Anton Kearsley and Terry Williams for help with analysis at the NHM (UK), Nikolay Karmanov and Sergey Kanakin for help with analysis at the Geological Institute SB RAS (Russia), Professor A.H. Rankin and Ms B. Beeskow for using the laser Raman equipment at Kingston University, UK. Ken Bailey, Alan Woolley, Ilya Veksler are thanked for useful discussions and information. Chris Stanley, Andy Fleet and Polly Hutchison helped to improve the text. Reviews by Keith Bell and an anonymous reviewer much improved the paper. The studies have been carried out with the support of the RFFR (grant 03-05-65270), Russian Science Support Foundation, Fund of Leading Scientific Schools of Russian Federation (NSch-2284.2003), a Royal Society (UK) incoming international short visit and INTAS grant 05-1000008-7938. This paper contributes to the list of 'CERCAMS' publications from The Natural History Museum.

References

Akaishi M, Kanda H, Yamaoka S (2000) Crystallization of diamond from C-O-H fluids under high-pressure and high-temperature conditions. J Cryst Growth 209:999–1003

Alberti A, Castorina F, Censi P, Comin-Chiaramonti P, Gomes CB (1999) Geochemical characteristics of Cretaceous carbonatites from Angola. J Afr Earth Sci 29:735–759

Bell K, Blenkinsop J (1989) Nd and Sr isotope geochemistry of carbonatites. In: Bell K (ed) Carbonatites: genesis and evolution. Unwin Hyman, London, pp 278–300

Bobrov AV, Litvin YuA, Divaev FK (2004) Phase relations and diamond synthesis in the carbonate of the Chagatai complex, Western Uzbekistan: results of P=4–7 GPa and T=1200–1700C. Geochem Int 42:39–48

Cartigny P, De Corte K, Shatsky VS, Ader M, De Paepe P, Sobolev NV, Javoy M (2001) The origin and formation of metamorphic microdiamonds from the Kokchetav massif, Kazakhstan: a nitrogen and carbon isotopic study. Chem Geol 176:265–281

Chiba H, Chacko T, Clayton RN, Goldsmidth JR (1989) Oxygen isotope fractionations involving diopside, forsterite and calcite: applications to geothermometry. Geochim Cosmochim Acta 53:2985–2995

Deines P (1989) Stable isotope variation in carbonatites. In: Bell K (ed) Carbonatites: genesis and evolution. Unwin Hyman, London, pp 301–359

Deines P (2002) The carbon isotope geochemistry of mantle xenoliths. Earth Sci Rev 58:247–278

Demény A, Ahijado A, Casillas R, Vennemann, TW (1998) Crustal contamination and fluid/rock interaction in the carbonatites of Fuerteventura (Canary Islands, Spain): a C, O, H isotope study. Lithos 44:83–151

Demény A, Sitnikova MA, Karchevsky PI (2004) Stable C and O isotope compositions of carbonatite complexes of the Kola Alkaline Province: phoscorite-carbonatite relationships and source compositions. In: Wall F, Zaitsev AN (eds) Phoscorites and carbonatites from mantle to mine: the key example of the Kola Alkaline Province, Mineralogical Society Series 10. Mineralogical Society, London, pp 407–431

Djuraev AD, Divaev FK (1999) Melanocratic carbonatites—new type of diamondbearing rocks, Uzbekistan. In: Stanley CJ et al (eds) Mineral deposits: processes to processing. Balkena, Rotterdam 1, pp 639–642

Dobretsov NL, Bulgatov AN (1991) Geodynamic map of Transbaikalia (concepts of preparation and legend) (in Russian). United Institute of Geology, Geophysics and Mineralogy and the Buryat Geological Institute SB RAS, Novosibirsk, p 51

Doroshkevich AG, Ripp GS (2004) The composition of magmas and fluids of carbonatite complexes of the Transbaikalia: data on study of inclusions. Extended abstracts of the interim IAGOD conference ''Metallogeny of the Pacific Northwest (Russian Far East): tectonics, magmatism and metallogeny of active continental margins'', Vladivostok, pp 288–292

Doroshkevich AG, Wall F, Ripp GS (2006) Calcite-bearing dolomite carbonatite dykes from Veseloe, North Transbaikalia, Russia and a discussion of the significance of their Cr-rich xenoliths. Mineral Petrol

Dunworth EA, Bell K (2001) The Turiy Massif, Kola Peninsula, Russia: isotopic and geochemical evidence for multi-source evolution. J Petrol 42:377–405

Faure G (1986) Principles of isotope geology. Wiley, New York, p 589

Ferrari AC, Robertson J (2001) Resonant Raman spectroscopy of disordered, amorphous, and diamondlike carbon. Phys Rev B 64:075414-1–075414-13

French BM, Rosenberg PE (1965) Siderite (FeCO3): thermal decomposition in equilibrium with graphite. Science 147:1283

Gellantly DC (1966) Graphite in natural and experimental carbonate systems. Mineral Mag 35:936–970

Gittins J, Harmer RE (1997) What is ferrocarbonatite? A revised classification. J Afr Earth Sci 25:159–168

Goldschmidt JR, Graf DL, Witters J, Northrop DA (1962) Studies in the system CaCO3-MgCO3-FeCO3: 1 Phase relations, 2 A method for major-element spectrochemical analysis, 3 Composition of some ferroan dolomites. J Geol 70:659–690

Harmer RE, Lee CA, Eglington BM (1998) A deep mantle source for carbonatite magmatism: evidence from the nephelinites and carbonatites of the Buhera district, SE Zimbabwe. Earth Planet Sci Lett 158:131–142

Kamenetsky MB, Sobolev AV, Kamenetsky VS, Maas R, Danyushevsky LV, Thomas R, Pokhilenko NP, Sobolev NV (2004) Kimberlite melts rich in alkali chlorides and carbonates: a potent metasomatic agent in the mantle. Geology 32:845–848

Karchevsky PI, Moutte J (2004) The phoscorite-carbonatite complex of Vuorijarvi, Kola Peninsula. In: Wall F, Zaitsev AN (eds) Phoscorites and carbonatites from mantle to mine: the key example of the Kola Alkaline Province, Mineralogical Society Series 10. Mineralogical Society, London, pp 163–199

Keller J, Hoefs J (1995) Stable isotope characteristics of recent natrocarbonatites from Oldoinyo Lengai. In: Bell K, Keller J (eds) Carbonatite volcanism: Oldoinyo Lengai and the petrogenesis of natrocarbonatites. IAVCEI Proceedings in Volcanology, vol 4. Springer, Berlin Heidelberg New York, pp 113–123

Krasnova NI, Petrov TG, Balaganskaya EG, Garcia D, Moutte J, Zaitsev AN, Wall F (2004) Introduction to phoscorites: occurrence, composition, nomenclature and petrogenesis. In: Wall F, Zaitsev AN (eds) Phoscorites and carbonatites from mantle to mine: the key example of the Kola Alkaline Province, Mineralogical Society Series 10. Mineralogical Society, London, pp 43–72

Kravtsov AI, Bobrov VA, Kropotkova OI (1981) Geochemistry of carbon of gases from kimberlites (in Russian). Abstracts of All-Union Symposium on geochemistry of carbon, Moscow, pp 73–76

Krivdik SG (2001) Alkaline magmatism of Ukraine shield. In: Vladykin NV (ed) Alkaline magmatism and the problem of mantle sources. Publishing house of the Institute of Geography SB RAS, Irkutsk, pp 46–58

Lee MJ, Garcia D, Moutte J, Williams CT, Wall F (2004) Carbonatites and phoscorites from the Sokli Complex, Finland. In: Wall F, Zaitsev AN (eds) Phoscorites and carbonatites from mantle to mine: the key example of the Kola Alkaline Province, Mineralogical Society Series 10. Mineralogical Society, London, pp 129–158

Litvin YuA (1998) Hot spots of mantle and experiment to 10 GPa: alkaline reactions, lithosphere carbonatization, and new diamond-generating systems. Russ Geol Geophys 39:1760–1768

Litvin YuA, Zharikov VA (2000) Experimental modelling of diamond genesis: diamond crystallization in multicomponent carbonate–silicate melts at 5–7 GPa and 1200–1570 °C. Dokl Earth Sci 373:867–871

Litvin YuA, Chudinovskikh LT, Sapari GV, Obyden SK, Chukichev MV, Vavilov VS (1999) Diamonds of new alkaline carbonate–graphite HP syntheses: SEM morphology, CCL-SEM and CL spectroscopy studies. Diamond Relat Mater 8:267–272

Lugovaya IP, Lapin AV, Krivdik SG (1980) A role of isotopic data for condition of formation of carbonatite complexes (in Russian). Abstracts of VIII All-Union Symposium on stable isotopes in geochemistry, pp 84–85

Luth RW (1993) Diamond, eclogites, and the oxidation state of the Earth's mantle. Science 261:66–68

Mourtada S, Le Bas MJ, Pin C (1997) Petrogenesis of Mg-carbonatites from Tamazert in the Moroccan High Atlas. CR Acad Sci II A 325:559–564

Nielsen TFD, Solovova IP, Veksler IV (1997) Parental melts of melilitolite and origin of alkaline carbonatite: evidence from crystallized melt inclusions, Gardiner complex. Contrib Mineral Petrol 126:331–344

Pal'yanov YuN, Sokol AG, Borzdov YuM, Khokhryakov AF, Sobolev NV (1999) Diamond formation from mantle carbonate fluids. Nature 400:417–418

Pal'yanov YuN, Sokol AG, Borzdov YuM, Khokhryakov AF, Sobolev NV (2002) Diamond formation through carbonate-silicate interaction. Am Mineral 87:1009–1013

Panina LI (2005) Multiphase carbonate-salt immiscibility in carbonate melts: data on melt inclusions from the Krestovskiy massif minerals (Polar Siberia). Contrib Mineral Petrol 150:19–36

Pasteris JD, Wopenka B (1991) Raman spectra of graphite as indicator of degree of metamorphism. Can Mineral 29:1–9

Pearson DG, Davies GR, Nixon PH, Milledge HJ (1989) Graphitized diamonds from a peridotite massif in Morocco and implications for anomalous diamond occurrences. Nature 338:60–62

Ripp GS, Badmatsyrenov MV, Doroshkevich AG (2003) Mineral composition and geochemical features of the Pogranichnoe carbonatites (North Transbaikalia). In: Vladykin NV (ed) Plumes and problems of deep sources of alkaline magmatism (in Russian). Publishing house of the Institute of Geography SB RAS, Irkutsk, pp 88–108

Ripp GS, Badmatsyrenov MV, Doroshkevich AG, Isbrodin IA (2004) Mineral composition and geochemical features of the Veseloe carbonatites (North Transbaikalia, Russia). In: Vladykin NV (ed) Plumes and problems of deep sources of alkaline magmatism. Publishing house of the Institute of Geography SB RAS, Irkutsk, pp 257–273

Ripp GS, Badmatsyrenov MV, Doroshkevich AG, Isbrodin IA (2005) New carbonatite-bearing area in Northern Transbaikalia. Petrology 13:489–498

Ripp GS, Karmanov NS, Doroshkevich AG, Badmatsyrenov MV, Izbrodin IA (2006) Chrome-bearing mineral phases in the carbonatites of Northern Transbaikalia. Geochem Int 44:395–403

Rosenberg PE (1963) Subsolidus relations in the system CaCO-FeCO3. Am J Sci 261:683–690

Santos RV, Clayton RN (1995) Variations of oxygen and carbon isotopes in carbonatites: a study of Brazilian alkaline complexes. Geochim Cosmochim Acta 59:1339–1352

Schrauder M, Navon O (1994) Hydrous and carbonatitic mantle fluids in fibrous diamonds from Jwaneng, Botswana. Geochim Cosmochim Acta 58:761–771

Spivak AV, Litvin YuA (2004) Diamond syntheses in multicomponent carbonate-carbon melts of natural chemistry: elementary processes and properties. Diam Rel Mat 13:482–487

Taylor HP, Frechen J, Degens ET (1967) Oxygen and carbon isotope studies of carbonatites from the Laacher See district, West Germany and the Alnö district, Sweden. Geochim Cosmochim Acta 31:407–430

Thompson RN, Smith PM, Gibson SA, Mattey DP, Dickin AP (2002) Ankerite carbonatite from Swartbooisdrif, Namibia: the first evidence for magmatic ferrocarbonatite. Contrib Mineral Petrol 143:377–396

Verwoerd WJ (1967) The carbonatites of South Africa and South West Africa. Handb GSSA 6:251–252

Vladykin NV, Morikiyo T, Miyazaki T (2004) Geochemistry of carbon and oxygen isotopes in carbonatites of Siberia and Mongoliya and some gedynamic consequences. In: Vladykin NV (ed) Deep-seated magmatism, its sources and their relation to plume processes. Publishing House of the Institute of Geography SB RAS, Irkutsk, pp 96–112

Vrublevskii VV, Pokrovskii BG, Zhuravlev DZ, Anoshin GN (2003) Composition and age of the penchenga linear carbonatite complex, Yenisei range. Petrology 11:130–147

Wada H, Suzuki K (1983) Carbon isotopic thermometry calibrated by dolomite-calcite solvus temperatures. Geochim Cosmochim Acta 47:697–706

Wall F (2000) Mineral chemistry and petrogenesis of rare earth-rich carbonatites with particular reference to the Kangankunde carbonatite, Malawi. PhD Thesis, University of London, p 340

Wall F, Zaitsev AN, Mariano AN (2001) Rare earth pegmatites in carbonatites. J Afr Earth Sci 32:A35–A36

Weidner JR, Tuttle OF (1965) Stability of siderite, $FeCO_3$. Geol Soc Am Spec Pap 82:220

Woolley AR, Kempe DRC (1989) Carbonatites: nomenclature, average chemical composition and element distribution. In: Bell K (ed) Carbonatites: genesis and evolution. Unwin Hyman, London, pp 1–46

Wopenka B, Pasteris JD (1993) Structural characterization of kerogens to granulite-facies graphite: applicability of Raman microprobe spectroscopy. Am Mineral 78:533–557

Worley BA, Cooper AF (1995) Mineralogy of the Dismal Nepheline Syenite, Southern Victoria Land, Antarctica. Lithos 35:109–128

Worley BA, Cooper AF, Hall CE (1995) Petrogenesis of carbonate-bearing nepheline syenites and carbonatites from Southern Victoria Land, Antarctica: origin of carbon and the effects of calcite-graphite equilibrium. Lithos 35:183–199

Zagnitko VN, Lugovaya IP, Proskurko LI (1980) Features of graphite from Ukraine on isotopic data (in Russian). Abstracts of Soviet-Union Symposium on stable isotopes in geochemistry, pp 314–315

Zuilen MA, Lepland A, Teranes J, Finarelli J, Wahlen M, Arrhenius G (2003) Graphite and carbonates in the 3.8 Ga old Isua Supracrustal Belt, southern West Greenland. Precambrian Res 126:331–348